Optimizing WAAS Accuracy/Stability For a Single Frequency Receiver

Euiho Kim, Todd Walter, J. David Powell, *Stanford University*

BIOGRAPHY

Euiho Kim is a Ph.D. candidate in the Aeronautics and Astronautics Department at Stanford University. He received his B.S. in Aerospace Engineering in 2001 from Iowa State University and his M.S. from Stanford University in 2002. His research currently focuses on precise positioning using a single frequency receiver and flight inspection truth systems.

Dr. Todd Walter received his B. S. in physics from Rensselaer Polytechnic Institute and his Ph.D. in 1993 from Stanford University. He is currently a Senior Research Engineer at Stanford University. He is a co-chair of the WAAS Integrity Performance Panel (WIPP) focused on the implementation of WAAS and the development of its later stages. Key contributions include: early prototype development proving the feasibility of WAAS, significant contribution to MOPS design and validation, co-editing of the Institute of Navigation's book of papers about WAAS and its European and Japanese counterparts, and design of ionospheric algorithms for WAAS. He was the co-recipient of the 2001 ION early achievement award.

Prof. J. David Powell received his B.S. degree in Mechanical Engineering from MIT and his Ph.D in Aero/Astro from Stanford in 1970. He joined the Stanford Aero/Astro Department Faculty in 1971 and is currently an Emeritus Professor. Recent focus of research is centered around applications of GPS: applications of the FAA's WAAS for enhanced pilot displays, the use of WAAS and new displays to enable closer spacing on parallel runways, and the use of WAAS for flight inspection for conventional navigation aids. He has co-authored two text books in control systems design.

ABSTRACT

The Wide Area Augmentation System (WAAS) provides accuracy (95%) to better than 1m in horizontal and 2m in vertical, which is quite an improvement compared to the stand-alone GPS accuracy and well within the WAAS specification. However, WAAS was designed and optimized for integrity rather than accuracy. Integrity requirements caused the selected carrier-smoothing time to be short and the weighting matrix for least-squares solutions to use overbounding variances. These choices are suboptimal for accuracy/stability. Even though the WAAS accuracy/stability is not optimized, airborne users accept this trade-off because integrity is critically related to safety. But, if one wants to use the WAAS for ground navigation, the same integrity requirements may not be necessary. Therefore, one can improve the WAAS accuracy/stability by relaxing the strict integrity specifications.

This paper investigates how to use the existing WAAS broadcast information to better optimize for accuracy and stability. First, we propose a new weighting matrix which appropriately represents the most likely signal conditions instead of using overbounding variances. Second, a method for dynamically adjusting the carrier smoothing time is investigated, which determines a right smoothing time based on the measurements of the rate of change of ionosphere. In addition to these methods, the Range Rate Correction (RRC) is removed, which is no longer necessary now that Selective Availability (SA) is permanently turned off. It has been observed that the RRC introduces noise with a 12 second period and 15~30 cm amplitudes in position domain. Overall, we expect that these methods improve the WAAS accuracy/stability and open a new way of using the WAAS for accuracy-oriented applications.

INTRODUCTION

When the Wide Area Augmentation System (WAAS) was designed, tremendous efforts were put into integrity because safety in using the WAAS for aviation must be guaranteed. The integrity required by the FAA is that the Vertical Protection Level (VPL) and the Horizontal Protection Level (HPL) must bound user position errors with the confidence of 99.99999%. Therefore, WAAS integrity equations are carefully constructed to ensure the integrity while satisfying more than 99.9% availability [1].

In WAAS, HPL and VPL are computed by using the overbounding variances of the residual errors, such as User Differential Range Error (UDRE) and Grid Ionospheric Vertical Error (GIVE), after applying WAAS corrections. Users take and adjust these variances with

their local position and combine them with the local receiver bounding variances to compute the VPL and the HPL as well as the weighting matrix which is used in computing position solutions [1]. This conservative way of computing integrity is essential for aviation users. However, if a user does not need to have such a high level of integrity in his/her application, there is a room for improvement in accuracy. In order to improve the WAAS accuracy for accuracy-oriented users, three methods are suggested in this paper: modifying the weighting matrix, adaptive carrier smoothing using code and carrier divergence (CCD) [2], and nullifying range rate correction (RRC).

First, a new weighting matrix is used instead of the weighting matrix in the WAAS MOPS in which the variances used in computing the weighting matrix in the WAAS are bounding variances. Since this weighting matrix typically does not represent the most likely current signal conditions, it may cause some errors in position solutions by discarding good measurements. Therefore, by modifying the weighting matrix to better represent current signal conditions, it may be possible to obtain more stable position solutions than the standard WAAS. A new weighting matrix uses more realistic variances for UDRE and GIVE and does not include any degradation terms.

Second, an adaptive carrier smoothing is proposed instead of using a fixed carrier smoothing time. This new method produces an optimal carrier smoothing time, which uses the code and carrier divergence (CCD) to estimate the ionospheric delay gradients and the level of noise including multipath and receiver noise [2]. Therefore, this method makes the carrier smoothing time robustly adapt to the current (10~15 min. time lag) ionospheric delay rate and noise level in order to result in smoother, more stable, and less biased position.

Third, the Range Rate Correction (RRC) is turned off. The RRC was designed to overcome the Selective Availability (SA). Although SA is permanently turned off, RRC is still implemented and most of time causes a 12 second periodic noise in position solutions [3]. Therefore, nullifying RRC will result in less noisy position than the WAAS without any harmful effects.

The three methods, modifying the weighting matrix, adaptive carrier smoothing using CCD, and nullifying RRC, will be discussed in detail. These algorithms are tested with static GPS data and WAAS correction messages. The test results will be given and analyzed. Finally, our conclusions will be presented.

MODIFYING WAAS WEIGHING MATRIX

A WAAS receiver shall use a weighting matrix to compute position. This weighting matrix is closely related to the WAAS protection level equations which uses the variance of Gaussian model distribution overbounding a true error distribution. The weighting matrix is diagonal and consists of a total variance, σ_i^2, which is the sum of the four error variances [4]

$$\sigma_i^2 = \sigma_{i,flt}^2 + \sigma_{i,UIRE}^2 + \sigma_{i,air}^2 + \sigma_{i,tropo}^2 \qquad (1)$$

where $\sigma_{i,flt}^2$ is the variance of fast and long term correction residuals, $\sigma_{i,UIRE}^2$ is the variance of ionospheric delay correction residuals, $\sigma_{i,air}^2$ is the variance of airborne receiver errors, and $\sigma_{i,tropo}^2$ is the variance of tropospheric error correction residuals.

Using the total variances for each satellite, the weighting matrix is constructed as followings.

$$W = \begin{bmatrix} \frac{1}{\sigma_1^2} & 0 & \cdots & 0 \\ 0 & \frac{1}{\sigma_2^2} & \cdots & 0 \\ \vdots & \vdots & \vdots & \vdots \\ 0 & 0 & \cdots & \frac{1}{\sigma_n^2} \end{bmatrix} \qquad (2)$$

It will be ideal if the weighting matrix closely represents true error variance. However, this weighting matrix most of time does not represent the current true error variance because each variance must be exaggerated to protect against possible unobserved large errors, which is the philosophy of the WAAS. Therefore, if the tight WAAS integrity requirement is relaxed, the weighting matrix can be modified to better represent true error variance for an accuracy oriented user. The weighting matrix can be modified as following discussions.

A. Modifying the Variance of Fast and Long Term Correction Residuals, σ_{flt}^2.

The variance of fast and long term correction residuals, $\sigma_{i,flt}^2$, is computed as described in [4].

$$\sigma_{flt}^2 = \begin{cases} (\sigma_{UDRE} \cdot \delta UDRE + \varepsilon_{fc} + \varepsilon_{rrc} + \varepsilon_{ltc} + \varepsilon_{er})^2, \\ \qquad \qquad \text{if } RSS_{UDRE} = 0 \\ (\sigma_{UDRE} \cdot \delta UDRE)^2 + \varepsilon_{fc}^2 + \varepsilon_{rrc}^2 + \varepsilon_{ltc}^2 + \varepsilon_{er}^2, \\ \qquad \qquad \text{if } RSS_{UDRE} = 1 \end{cases} \qquad (3)$$

where RSS$_{UDRE}$ is root-sum-square flag in Message Type 10. σ_{UDRE} is the standard deviation of User Differential Range Error (UDRE) from Message Type 2-6 and 24. $\delta UDRE$ is a location-specific modifier for σ_{UDRE} [5]. ε_{fc}, ε_{rrc}, ε_{ltc} and ε_{er} are the degradation parameters for fast correction data, range rate correction data, long term correction or GEO navigation message data, and en route through NPA (Non-precision approach) applications.

σ_{UDRE} is evaluated from UDRE indicator (UDREI$_i$) provided from Message Type 2-6 and 24. The conversion table in the WAAS MOPS from the UDREI to σ_{UDRE} is shown in Table 1. In Table 1, a new UDRE variance table is also shown, which is obtained from the statistics of post-processed user differential range errors without ionospheric delays corresponding to each UDREI. Compared to the MOPS UDRE variance, the new UDRE variance is much smaller because it does not conservatively bound errors but rather is close to the true error variance.

UDREI	UDRE	MOPS UDRE Variance(m^2)	New UDRE Variance (m^2)
0	0.75	0.0520	0.0260
1	1.0	0.0924	0.0296
2	1.25	0.1444	0.0332
3	1.75	0.2830	0.0368
4	2.25	0.4678	0.0404
5	3.0	0.8315	0.0633
6	3.75	1.2992	0.0892
7	4.5	1.8709	0.1169
8	5.25	2.5465	0.154
9	6.0	3.3260	0.216
10	7.5	5.1968	0.275
11	15.0	20.787	0.512
12	50.0	230.9661	0.600
13	150.0	2078.695	5.40
14	NM	-	-
15	DNU	-	-

Table 1: New evaluation of UDREI

In addition to the new UDRE variances, σ_{flt}^2 can be improved by ignoring the correction degradation variances which include ε_{fc}, ε_{rrc}, ε_{ltc} and ε_{er} because the fast and long term errors typically grow much slower than the degradation factors. $\delta UDRE$ is set to unity because the ephemeris errors it is designed to protect against rarely occur.

Designating the new UDRE variance as $\sigma_{New\_UDRE}^2$, the new variance of fast and long term correction residuals can be simplified as follows.

$$\hat{\sigma}_{flt}^2 = \hat{\sigma}_{New\_UDRE}^2 \qquad (4)$$

B. Modifying the Variance of User Ionospheric Range Error, σ_{UIRE}^2 .

When WAAS-based ionospheric delay corrections are applied to a user, the variance of user ionospheric range error is computed as follows [4].

$$\sigma_{UIRE}^2 = F_{pp}^2 \cdot \sigma_{UIVE}^2 \qquad (5)$$

where F_{pp} is the obliquity factor and σ_{UIVE}^2 is the variance of User Ionospheric Vertical Error (UIVE).

The WAAS MOPS states that the computation of σ_{UIVE}^2 shall include the degradation of ionospheric corrections, ε_{iono} . Again, this degradation factor is ignored since ionospheric delay correction typically degrade much slower than ε_{iono} .

Then, σ_{UIVE}^2 can be computed as followings.

$$\sigma_{UIVE}^2 = \sum_{n=1}^{N} W_n \cdot \sigma_{n,GIVE}^2 \qquad (6)$$

where W is a weighting factor which is a function of Ionosphere Piece Point (IPP). N is the number of Ionosphere Grid Point (IGP) used for the interpolation of ionosphere vertical delay at an IPP. σ_{GIVE}^2 is the variance of Grid Ionosphere Vertical Error (GIVE) and is evaluated from the Grid Ionosphere Vertical Error Indicator (GIVEI) sent by Message Type 26.

Like σ_{UDRE} , σ_{GIVE} in the MOPS is very conservative. Table 2 compares the GIVE variance in the MOPS, σ_{GIVE}^2 , and the new GIVE variance, $\hat{\sigma}_{New\_GIVE}^2$.

$\hat{\sigma}_{New\_GIVE}^2$ is again computed from the statistics of post-processed residual Grid Ionospheric Vertical Error corresponding to each GIVEI. It better represents the residual errors most of time but can't be used for the integrity that the WAAS requires.

GIVEI	GIVE	MOPS Variance(m^2)	New Variance (m^2)
0	0.3	0.0084	0.0084
1	0.6	0.0333	0.0136
2	0.9	0.0749	0.0187
3	1.20	0.1331	0.0210
4	1.5	0.2079	0.0230
5	1.8	0.2994	0.0255

6	2.1	0.4075	0.0272
7	2.4	0.5322	0.0289
8	2.7	0.6735	0.0306
9	3.0	0.8315	0.0323
10	3.6	1.1974	0.0432
11	4.5	1.8709	0.0675
12	6	3.3260	0.110
13	15	20.787	0.304
14	45	187.0826	0.951
15	NM	-	-

Table 2: New evaluation of GIVEI

Therefore, a new variance of user ionospheric range error is computed as follows.

$$\hat{\sigma}_{UIRE}^2 = F_{pp}^2 \cdot \hat{\sigma}_{New\_UIVE}^2 \qquad (7)$$

where

$$\hat{\sigma}_{New\_UIVE}^2 = \sum_{n=1}^{N} W_n \cdot \hat{\sigma}_{n,New\_GIVE}^2 \qquad (8)$$

C. Modifying the Variance of Airborne Receiver Errors

In [4], the variance of airborne receiver errors is computed as follows.

$$\sigma_{air}^2[i] = \sigma_{noise}^2[i] + \sigma_{multipath}^2[i] + \sigma_{divg}^2[i] \qquad (9)$$

where

$$\sigma_{multipath}[i] = 0.13 + 0.53e^{(-\theta[i]/10°)} \ \left(\text{in meters}\right) \quad (10)$$

$\theta[i]$ is the elevation angle of i satellite in degrees. σ_{divg} is defined as the difference between the induced error at the steady-state responses of a implemented carrier smoothing filter and the standard filter which uses 100s as a smoothing window. The difference shall be greater than zero if the implemented filter uses a different smoothing time. σ_{noise} is the standard deviation of a normal distribution which bounds the errors associated with a GNSS receiver noise such thermal noise.

σ_{air} bounds the remaining receiver noises and airborne multipath after the carrier smoothing. Not only σ_{air} is very conservative, but it is designed for an airborne user. In this paper, this term is replaced by $\hat{\sigma}_{RN\_M}$ computed based on the observation of ionospheric delay slope, receiver noise and multipath using code and carrier divergence (CCD). Carrier smoothing time also effects $\hat{\sigma}_{RN\_M}$, therefore the detailed procedure in finding $\hat{\sigma}_{RN\_M}$ will be described in the below section.

ADAPTIVE CARRIER SMOOTHING USING CODE-CARRIER DIVERGENCE (CCD)

This section introduces a new way of determining a carrier smoothing time for a single frequency receiver proposed in [2]. The carrier smoothing time of the nominal filter defined in [4] is 100 seconds. This specific value is determined from considering the bounding rate of ionospheric delays during a nominal day. However, if ionospheric delay gradients and the level of multipath and receiver noise can be estimated, then a constant smoothing time does not need to be used. Instead, a smoothing time can adaptively change according to those estimates to obtain a better stability than a fixed carrier smoothing. This section summarizes how to determine an optimal carrier smoothing time based on the estimates of the rate of ionospheric delays, receiver noise and multipath using the code and carrier divergence (CCD). Then, the computation of $\hat{\sigma}_{RN\_M}$ will be shown.

A. Estimation of Ionospheric Delay Gradients, Receiver Noise and Multipath Using CCD

The basic measurements in a GPS receiver are code and carrier phase measurements. The code phase measurements, ρ, and the carrier phase measurements, Φ, can be written as

$$\rho = r + c[\delta t_u - \delta t_s] + I + T + M_\rho$$
$$\Phi = r + c[\delta t_u - \delta t_s] - I + T + N + M_\Phi \qquad (11)$$

where r is the true range between a receiver and a satellite. c is the speed of light. δt_u and δt_s are a receiver and satellite clock errors. I is ionospheric delay and T is tropospheric delay. N is the integer ambiguity. M_ρ and M_Φ includes multipath, thermal noises, and modeling errors in the code and carrier phase measurements respectively.

The difference of code and phase measurements gives the following equation.

$$y_t = \rho_t - \Phi_t$$
$$= 2I_t - N + M_{t,\rho} - M_{t,\Phi} \qquad (12)$$

It should be noted that ionospheric delays slowly change with respect to time during nominal ionospheric days. Therefore, the gradients can be seen as a constant during a short time window (tens of minutes). The mean-subtracted y_t can be rewritten as

$$\tilde{y}_t = 2a \cdot t + b + M_{t,\rho} \qquad (13)$$

where a is a rate of ionospheric delay. b is an arbitrary constant. In equation (13), M_{Φ} is ignored because it is much smaller than M_{ρ} which is zero-mean over time.

Expressing the time series of equation (13) in a matrix form yields

$$\underbrace{\begin{bmatrix} \tilde{y}_{t_1} \\ \tilde{y}_{t_2} \\ \vdots \\ \tilde{y}_{t_n} \end{bmatrix}}_{Y} = \underbrace{\begin{bmatrix} 2 \bullet t_1 & 1 \\ 2 \bullet t_2 & 1 \\ \vdots \\ 2 \bullet t_n & 1 \end{bmatrix}}_{T} \underbrace{\begin{bmatrix} a \\ b \end{bmatrix}}_{X} + \underbrace{\begin{bmatrix} M_{t_1,\rho} \\ M_{t_2,\rho} \\ \vdots \\ M_{t_n,\rho} \end{bmatrix}}_{M}$$

$$\tilde{Y} = TX + M \qquad (14)$$

Now, the problem becomes to find a in the presence of $M_{t,\rho}$. If $M_{t,\rho}$ is close to white nose, the ordinary least-squares (OLS) is a right choice in estimating a. However, if $M_{t,\rho}$ is highly correlated, the generalized least-squares (GLS) is recommended to be used [6].

The OLS solution of equation (14) is

$$X_O = (T'T)^{-1}T'Y \qquad (15)$$

The GLS solution of equation (14) is

$$X_G = (T'\Sigma^{-1}T)^{-1}T'\Sigma^{-1}Y \qquad (16)$$

where Σ is the covariance matrix of M.

The generalized least square (GLS) requires covariance matrix of the noise to estimate X_G. However, the covariance matrix is usually unknown. Therefore, it is necessary to estimate the covariance matrix and the X_G at the same time. This is well-known problem in econometrics and solved by using 2 step process [6]. This subject is not discussed in this paper, but a great deal of the procedure is discussed in [6]

Figure 1 shows a typical pattern of $\tilde{y}_t$ with an estimated trend by using GLS.

Once X_G is estimated, the receiver noise and multipath can be separated from ionospheric delays and an integer ambiguity as followings.

$$\hat{M} = \tilde{Y} - T\hat{X}_G \qquad (17)$$
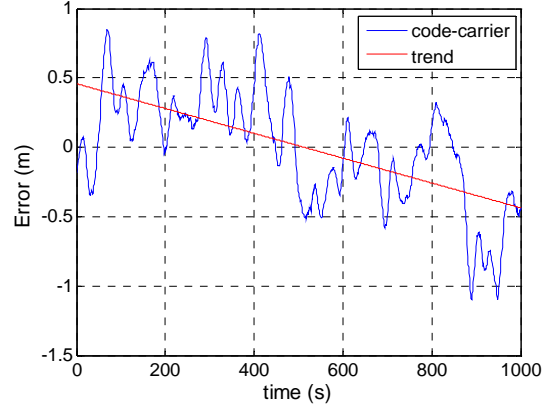
Figure 1: Mean subtracted difference of code and carrier phase measurements

B. Determination of Optimal Carrier Smoothing Time

Using the Hatch filter, the carrier-smoothed pseudorange at time t, $\bar{\rho}_t$, is given by

$$\bar{\rho}_t = \tfrac{1}{k}\rho_t + \tfrac{k-1}{k}(\bar{\rho}_{t-1} + \Phi_t - \Phi_{t-1}) \qquad (18)$$

where k is a carrier smoothing time.

The error, ε, in the smoothed pseudorange measurements can be described as [7]

$$\varepsilon_t = \bar{\rho}_t - c[\delta t_u - \delta t_s]_t - I_t - T_t \qquad (19)$$

If the ionospheric delay slope can be assumed to be constant, then the steady state error, ε, can be described as follows [2].

$$\varepsilon_t = -2(k-1)a + \frac{1}{k}\sum_{i=0}^{t-1}\left(\frac{k-1}{k}\right)^i M_{t-i} \qquad (20)$$

From equation (20), it should be noted that the steady state error, ε, of the carrier smoothing filter is a function of the rate of ionospheric delays, receiver noise and multipath in the code phase measurements, and a carrier smoothing time. The trade-off of using the hatch filter is that the lager the carrier smoothing time, there is a bigger bias and lesser effects of multipath in ε.

Based on ε, a cost function, which is only a function of the k, once a and M are estimated, can be expressed in two forms according to multipath characteristics: white noise and quasi sinusoidal wave.

Equation (21) shows a proposed cost function, J_w, when multipath can be assumed to be white noise.

$$J_w(k,a,\sigma) = 4(k-1)^2 a^2 + \mu \frac{\sigma_{M_W}^2}{2k-1} \qquad (21)$$

where σ is the standard deviation of M_W and μ is a weighting factor. Equation (21) is the sum of the square of the first term and the variance of the second term in equation (20).

On the other hand, when multipath is highly correlated or quasi sinusoidal, the following cost function is proposed.

$$J_s = 4(k-1)^2 a^2 + \frac{\mu(2\sigma_{M_S})^2}{k^2(1-2\phi\cos(\omega)+\phi^2)} \qquad (22)$$

where $\phi = \frac{k-1}{k}$. ω is the lowest distinct radial frequency component of M_S which can be found by Fourier transform. The square root of the second term of J_s is the maximum value of the steady state response when $M_{S,t} = (2\sigma_{M_S})\cos(wt)$ at time t. This specific maximum value is chosen because it mostly bounds the steady state response of a quasi sinusoidal wave. Figure 2 shows the steady-state response of the given time series of multipath and receiver noise and its expected bound after carrier smoothing. The time series of multipath and receiver noise used in the figure are separated from CCD using the GLS procedure.
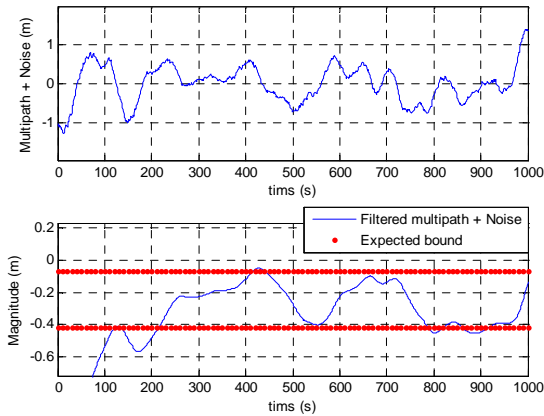

Figure 2: Expected bound to the stead-state response of quasi-sinusoidal multipath and noise

An optimal carrier smoothing time, k_{opt}, can be computed, from the cost functions, J_w and J_s with the tuning factor, μ. For example, Figure 3 shows the k_{opt} values computed from J_s with different levels of the rate of ionospheric delay and receiver noise and multipath when $\mu = 2$ and $\omega = 0.04 rad$. This value of ω is

chosen based on observations. The tuning factor μ used for Figure 3 is set to 2 so that the induced error is less than 2m with a noise amplitude up to 5m and an ionospheric delay rate up to 8 mm/s which bounds the rate of ionospheric delays during nominal days [7]. The corresponding cost J_{opt} of k_{opt} is shown Figure 4.
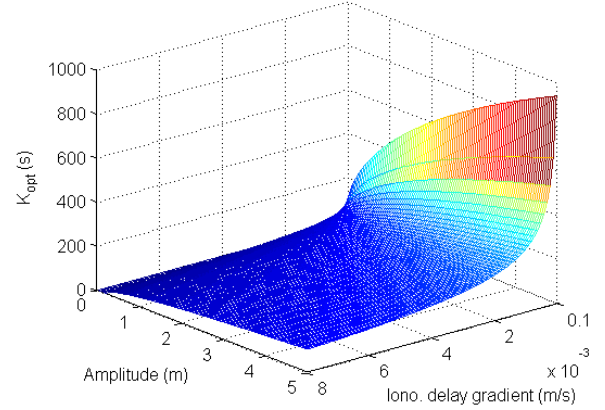
Figure 3: The optimal k for sinusoidal multipath given noise amplitude and ionospheric delay rate
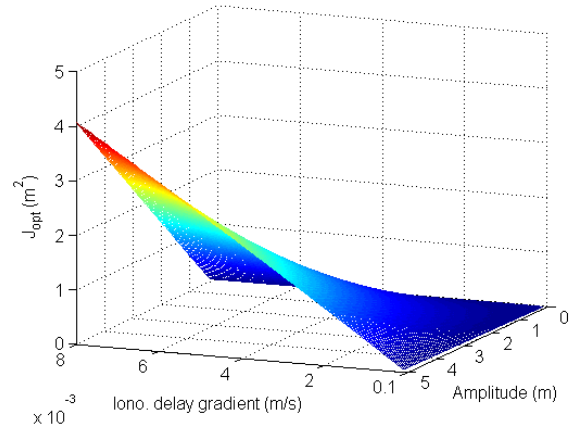
Figure 4: Induced error corresponding to the optimal k give noise amplitude and ionospheric delay rate

Again, readers can found more rigorous discussion and derivation in [2].

After k_{opt} is chosen from minimizing J_w and J_s, $\hat{\sigma}_{RN\_M}$ can be obtained by substituting k_{opt} back to equation (21) and (22). $\hat{\sigma}_{RN\_M_W}$ for white noise multipath is computed as follows.

$$\hat{\sigma}_{RN\_M_W} = 4(k_{opt}-1)^2 a^2 + \frac{\sigma^2}{2k_{opt}-1} \qquad (23)$$

$\hat{\sigma}_{RN\_M_S}$ for sinusoidal multipath is computed as follows.

$$\hat{\sigma}_{RN\_M_S} = 4(k_{opt}-1)^2 a^2 + \frac{(2\sigma)^2}{k_{opt}^2(1-2\phi_{opt}\cos(\omega)+\phi_{opt}^2)} \quad (24)$$

where $\phi_{opt} = \dfrac{k_{opt}-1}{k_{opt}}$.

NULLYFYING RANGE RATE CORRECTION

When WAAS was developed, the range rate correction, *RRC*, was designed to overcome Selective Availability (SA) which is now permanently turned off. However, WAAS receivers still apply *RRC* because it is required in [4]

The range rate correction, *RRC*, is computed by a user as follows.

$$RRC(t_{of}) = \frac{PRC_{current} - PRC_{previous}}{\Delta t} \quad (25)$$

where *PRC* is the fast corrections and t_{of} is the time of applicability. Δt is the time difference between $PRC_{current}$ and $PRC_{previous}$.

RRC makes the pseudorange correction have periodic noise. This cyclic noise basically has a 12 second period, but this cyclic pattern is not always consistent. Figure 5 shows the example of fast corrections with RRC frozen over time.
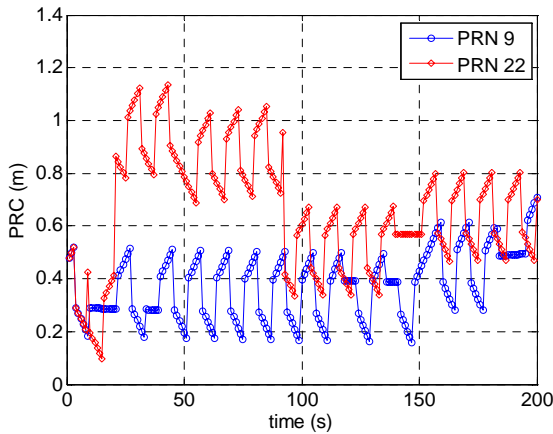

Figure 5: Behavior of RRC of PRN 9 and 22

WAAS position solutions have the similar noise pattern as shown in Figure 6. Therefore, turning off the RRC result in better performance.
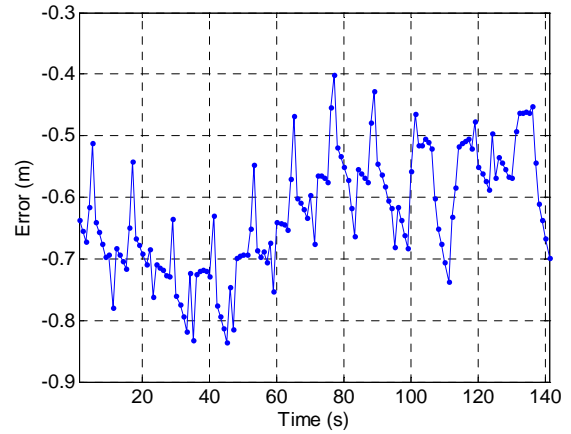

Figure 6: Effect of RRC in a position domain

RESULTS

The proposed methods are tested on the static data taken at Stanford University on September 6, 2006. The effect of the new weighting matrix will be discussed first, then how the three proposed methods improve the accuracy/stability of the WAAS will be shown.

### A. Effect of the New Weighting Matrix

Figures 7 and 8 compare the east and up position errors from the standard WAAS and the optimized WAAS with a new weighting matrix. Figures 9 and 10 show the total variances for the standard WAAS and the optimized WAAS. There are significant positioning improvements when the time is near 3000 seconds and around 6000 seconds. The position from the optimized WAAS with the new weighting matrix shows better stability around these times. The variances in Figures 9 and 10 explain why the new weighting matrix results in better stability. The two of the total variances in Figure 9 are much larger than the rest of the variances near the 3000 seconds and the one variance is also larger than the rest around the 6000 seconds. The satellites with these large variances are heavily de-weighted so that they are effectively excluded in computing position. On the other hand, the new total variances in Figure 10 show that the difference of these variances is not as extreme as the WAAS variances in Figure 9. Therefore, the satellites that have a large variance are relatively less de-weighted than the standard WAAS and help to obtain better position solutions.
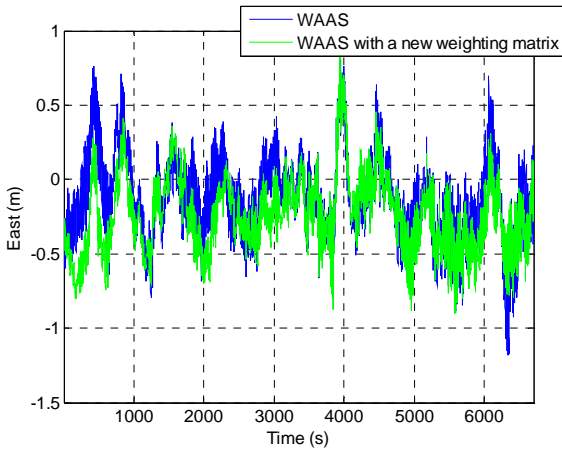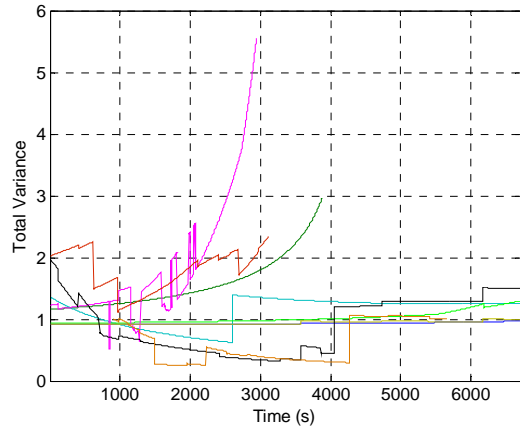
Figure 7: Comparison of the position errors in east from the standard WAAS and the WAAS with a new weighting matrix
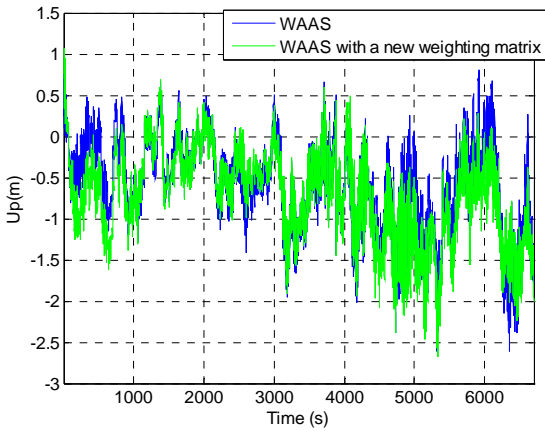
Figure 8: Comparison of the position errors in up from the standard WAAS and the WAAS with a new weighting matrix
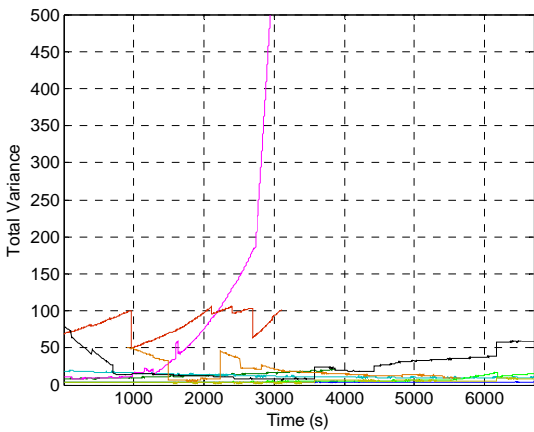

Figure 9: Total variance from the standard WAAS


Figure 10: Total variance from the optimized WAAS

B. Overall Improvements

Figures 11 and 12 compare the position errors from the standard WAAS, optimized WAAS with 100s carrier smoothing time, and optimized WAAS with the adaptive carrier smoothing time. For adaptive carrier smoothing, a 1000 seconds window of code minus carrier measurements and $\hat{\sigma}_{RN\_M_W}$ are used. The two plots show that the optimized WAAS with adaptive carrier smoothing effectively reduce multipath without suffering a noticeable induced bias. Terminating RRC further reduces the noise. Overall the optimized WAAS with adaptive carrier smoothing produces significantly better stability than the standard WAAS and the optimized WAAS with 100s carrier smoothing.
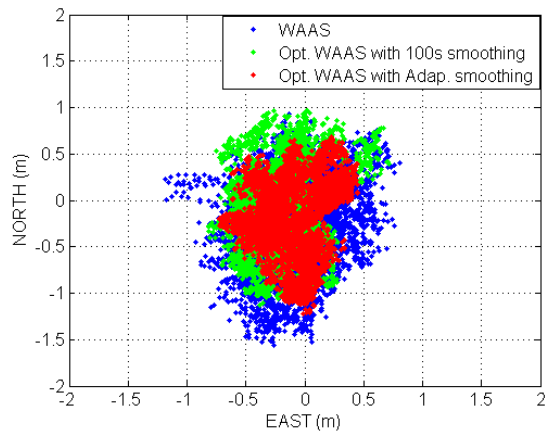
Figure 11: Comparison of the horizontal errors the standard WAAS and the Optimized WAAS with 100s and

adaptive smoothing time
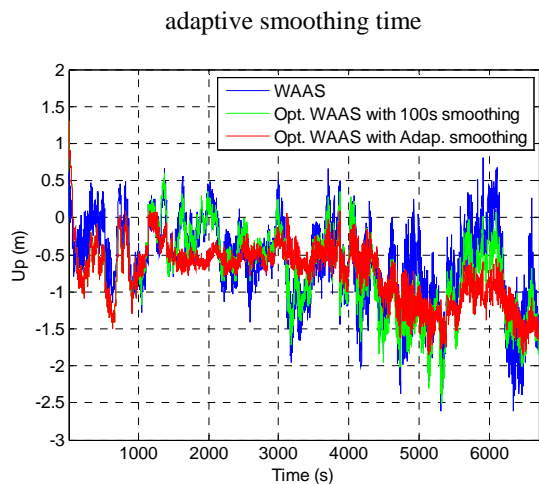
Figure 12: Comparison of the vertical errors the standard WAAS and the Optimized WAAS with 100s and adaptive smoothing time

CONCLUSION

The standard WAAS was optimized for accuracy and stability by applying a new more realistic weighting matrix, removing range rate correction (RRC), and using adaptive carrier smoothing. The results show that the proposed three methods significantly improve WAAS stability and slightly improve accuracy. The new weighting matrix produces more stable positions particularly when some satellites have significantly (50 to 100 times) larger total variance than the others.

ACKNOWLEDGMENTS

The authors gratefully acknowledge the support of FAA flight inspection division (AVN)

REFERENCES

[1] Walter, T., P. Enge and A.Hansen, "A Proposed Integrity Equation for WAAS MOPS", in Proceedings of ION GPS Meeting 1997

[2] Euiho Kim, "Apaptive Carrier Smoothing Using Code and Carrier Divergence (CCD) ", to be published in ION-NTM 2007

[3] E. Kim, T. Walter, and J.D. Powell, " A Development of WAAS-Aided Flight Inspection Truth System", in Proceedings of IEEE/ION PLANS 2006

[4] Minimum Operational Performance Standards for Global Positioning System/Wide Area Augmentation System Airborne Equipment. Washington, D.C, RTCA SC-159, WG-2, DO-229C, 28 Nov, 2001.

[5] T. Walter, A. Hansen, and P. Enge, " Message Type 28", in Proceeding of ION NTM 2001

[6] P.J. Brockwell, and R.A. Davis, "Introduction to Time Series and Forecasting", second edition, Springer, 2002

[7] T. Walter et al., "The Effects of Large Ionospheric Gradients on Single Frequency Airborne Smoothing Filters for WAAS and LAAS", in Proceeding of ION NTM 2004